Effect of Vacuum on Lignocellulosic Biomass Flash Pyrolysis in a Conical Spouted Bed Reactor

ARTICLE *in* ENERGY & FUELS · SEPTEMBER 2011

Impact Factor: 2.79 · DOI: 10.1021/ef200712h

energy&fuels

ARTICLE

pubs.acs.org/EF

Effect of Vacuum on Lignocellulosic Biomass Flash Pyrolysis in a Conical Spouted Bed Reactor

Maider Amutio, Gartzen Lopez, Roberto Aguado, Maite Artetxe, Javier Bilbao, and Martin Olazar*

Department of Chemical Engineering, University of the Basque Country, Post Office Box 644, E48080 Bilbao, Spain

ABSTRACT: The continuous flash pyrolysis of lignocellulosic biomass under atmospheric and vacuum conditions (0.25 atm) has been studied in a bench-scale plant provided with a conical spouted bed reactor. A previous kinetic study has been carried out in thermobalance, and the kinetic data have been fitted to a three parallel and independent reaction model by deconvolution of the differential thermogravimetry (DTG) curve. The influence of vacuum on product yields, compositions, and properties has been carried in a bench-scale plant at 400 and 500 °C. Vacuum operation in a conical spouted bed is advantageous for biomass pyrolysis because of the reduction in the N_2 mass flow rate required for the spouted bed regime. Consequently, the energy requirements for heating N_2 and the problems related to the condensation of the outlet stream are significantly reduced. The yields obtained and the composition of the bio-oil provide evidence that the vacuum operation does not affect the good gas−solid contact and the excellent performance of the conical spouted bed reactor for lignocellulosic biomass flash pyrolysis. High bio-oil yields are obtained, 77% at 500 °C and under 0.25 atm. Vacuum leads to a slightly heavier and less oxygenated bio-oil and a char fraction with improved surface characteristics.

1. INTRODUCTION

There is an urgent need to find alternative raw materials to fossil fuels because of falling oil reserves and a rising demand for energy, automotive fuels, raw materials for the current petrochemical industry, and H_2. Accordingly, lignocellulosic biomass is the only renewable source of fixed carbon that can be converted into liquid, solid, and gaseous fuels, apart from heat and power, with no contribution to the net emission of CO_2. Pyrolysis is one of the technologies with the best industrial perspectives for this valorization, because the process conditions can be optimized to maximize the yields of gases, liquids, or chars.[1,2]

The production of a liquid fraction or bio-oil by means of lignocellulosic biomass flash pyrolysis has received growing interest because of the perspectives of bio-oil as a feed for refinery units (biorefinery).[3] Thus, it is possible to decouple bio-oil production in rural areas and on a moderate scale from its upgrading in either refinery units to obtain transportation fuels and valuable chemicals or large power plants to convert it into heat and power.[4−6] The refinery units attracting more attention for bio-oil co-feeding are fluidized catalytic cracking (FCC) units[7−9] and the methanol to olefin (MTO) process.[10]

Flash pyrolysis maximizes the bio-oil yield and is carried out at moderate temperatures (around 500 °C) with short vapor residence times (typically below 1 s) and high heating rates, 10^3−10^4 °C s^{-1}. These characteristics maximize the bio-oil yield, given that secondary cracking reactions are minimized.[11,12] Furthermore, char must be rapidly withdrawn from the reaction environment, because hot char is catalytically active for cracking organic vapors.[13] The flash pyrolysis of biomass produces bio-oil yields typically in the 60−80 wt % range, a gas yield of 10−20 wt %, and a char yield in the 15−25 wt % range.[11−13] Gas is mainly composed of CO_2 and CO; therefore, its heating value is relatively low, but it can be used to supply energy to the pyrolysis plant. Char can be used as fuel, owing to its high heating value, can be subjected to activation processes to obtain active carbon for purification processes, and can also be used as a support for metallic or acid catalysts.[14−19] In addition, biomass pyrolysis char has the potential for soil amendment because of long-term carbon sequestration in the soil.[20]

A wide range of reactor configurations has been used to perform biomass flash pyrolysis, such as fluidized-bed reactors,[21−23] transport and circulating fluidized-bed reactors,[24,25] ablative reactors (rotating and cyclonic),[26] auger reactors,[27] and vacuum reactors.[28] The conical spouted bed reactor (CSBR), which is an alternative to fluidized beds, is of proven suitability for biomass flash pyrolysis.[29,30] Particle cyclic movement allows for the handling of particles of irregular texture, fine particles, sticky solids, and those with a wide size distribution, with no segregation and agglomeration problems.[31,32] Furthermore, the great versatility concerning the gas flow rate allows for operation with short gas residence times (as low as milliseconds) in the dilute spouted bed regime.[33] The vigorous particle cyclic movement and the high inert gas flow rate contribute to a high heating rate and high heat- and mass-transfer rates between phases.[34] Calonaci et al.[35] have confirmed that the bio-oil yield obtained in the CSBR is close to the maximum obtainable yield predicted by their macrokinetic model. In addition, the CSBR is appropriate for continuous operation, which is especially relevant for the implementation of large-scale biomass flash pyrolysis with the additional advantage of a simple design.

Biomass flash pyrolysis under vacuum improves the operational capacity of this technology by enhancing certain requirements: (i) it decreases the mass flow rate of inert gas, and consequently, less energy is required to heat the inert gas to the

Received: May 13, 2011
Revised: July 27, 2011
Published: July 28, 2011

Table 1. Biomass Characterization

Ultimate Analysis (wt %)	
carbon	49.33
hydrogen	6.06
nitrogen	0.04
oxygen	44.57
Proximate Analysis (wt %)	
volatile matter	73.4
fixed carbon	16.7
ash	0.5
moisture	9.4
HHV (MJ kg^{-1})	19.8

reaction temperature, and (ii) the collection of the bio-oil is easier, because pyrolytic volatile products have similar properties to cigarette smoke and are very difficult to condensate.[13]

In addition, vacuum biomass pyrolysis minimizes secondary cracking reactions because of the rapid desorption and extraction of the volatile products from the reaction environment.[36] Another advantage of vacuum operation is the improvement in char quality, whose surface area increases, given that the undesirable processes of volatile carbonization by secondary reactions are minimized during vacuum operation.[37]

The most relevant papers related to vacuum pyrolysis in terms of the scale and technology transfer achieved are those published by Laval University with the Pyrovac process using a moving bed reactor.[28,36−45] In this reactor, the main role of the vacuum is to enhance the outflow of the volatiles from the reactor.

In a previous paper, Lopez et al.[46] proved the suitability of the CSBR for vacuum operation in the pyrolysis of waste tires, concluding that this reactor performs well in the vacuum pyrolysis of tire material. Furthermore, vacuum increases the yield of the liquid fraction corresponding to diesel fuel and improves the surface area of the residual carbon black. Previously, Lopez et al.[47] studied in thermobalance the influence of pressure on the pyrolysis of tires and observed that vacuum slightly improves the kinetics of the pyrolysis process, even at low temperatures and at the initial stages of the reaction.

In this study, a CSBR has been used for pinewood sawdust flash pyrolysis under vacuum and with continuous feed to prove the aforementioned operational advantages and compare product yields and compositions to those obtained in a previous paper using the same technology by continuously feeding the sawdust under ambient pressure.[30] In addition, a kinetic study has been carried out in a thermogravimetric analyzer to establish the effect of the pressure on the pyrolysis kinetics.

2. EXPERIMENTAL SECTION

2.1. Raw Material. The biomass used in this study is forest pinewood waste (*Pinus insignis*). This material has been crushed and ground to a particle size in the 1−2 mm range and dried to a moisture content below 10 wt %. Ultimate and proximate analyses have been carried out in a LECO CHNS-932 elemental analyzer and in a TGA Q500IR thermogravimetric analyzer, respectively. The higher heating value (HHV) has been measured in a Parr 1356 isoperibolic bomb calorimeter. The main characteristics of the raw biomass are summarized in Table 1.

2.2. Runs for Kinetic Study. The kinetic study has been carried out in a TGA Q500IR thermobalance. The operating method involves subjecting the sample (approximately 0.01 g) to a heating ramp of 15 °C min^{-1} from room temperature to 800 °C, in an inert atmosphere (N_2) with a flow rate of 0.1 NL min^{-1} under two different absolute pressures: 1 and 0.25 atm.

2.3. Pyrolysis Pilot Plant and Experimental Procedure. A continuous pyrolysis unit has been set up and fine-tuned (Figure 1) based on the hydrodynamic studies carried out in a cold unit[48,49] and in a unit at pyrolysis temperatures and under subatmospheric pressures[50] and the experience acquired in the pyrolysis of biomass[29,30] and other types of wastes, such as tires[51,52] and plastic wastes.[53−55] Furthermore, the excellent performance of the CSBR has been confirmed in the scale-up of the biomass pyrolysis process to a 25 kg h^{-1} pilot plant.[34] The problems and limitations related to bed stability in the CSBR at a larger scale have been overcome using internal devices that lead to a more stable operation and lower gas flow rate and pressure drop.[56]

The feeding system, which is pneumatically actuated, allows for the continuous feeding of the biomass and is able to feed up to 3.3 g min^{-1} of sawdust. The nitrogen flow is controlled by a mass flow meter that permits feeding up to 30 L min^{-1} and is heated to the reaction temperature by means of a preheater.

The CSBR consists of a lower conical section and an upper cylindrical section, and its total height is 0.34 m. The height of the conical section is 0.205 m, and the angle of the conical section is 28°. The diameter of the cylindrical section is 0.123 m. The bottom diameter is 0.02 m, and the gas inlet diameter is 0.01 m. Further information on the reactor can be found elsewhere.[52] The CSBR allows for continuous operation by selectively removing the char from the bed, which avoids its accumulation throughout the pyrolysis process. The fountain region of the CSBR is characterized by the segregation of different density materials, where the solids of lower density (char) describe higher trajectories, circulating near the reactor wall and allowing for the removal of the char through a lateral pipe (Figure 2).[31,57]

The volatile products leave the reactor together with the inert gas and pass through a high-efficiency cyclone followed by a 25 mm sintered steel filter, both placed at a hot box maintained at 280 °C to prevent the condensation of heavy compounds. The vapor residence time within the fine-particle retention system is less than 1 s, avoiding the partial cracking of the vapors before their condensation. The gases leaving this filter circulate through a volatile condensation system, consisting of a condenser and two coalescence filters. The condenser is a double shell tube cooled by tap water, and the coalescence filters ensure the condensation of the aerosols remaining in the gas stream. Accordingly, the liquid collected in the condenser is mostly the aqueous phase of the bio-oil, whereas the heavier compounds that make up the organic phase are retained in the coalescence filters.

Vacuum is attained in the plant by means of a Vacuubrand MZ2D vacuum pump placed downstream of the coalescence filters. The pressure within the reactor is controlled by means of a needle valve placed between the reactor and the pump. It is noteworthy that vacuum can be easily obtained with this technology, where a low dead volume is required in the reactor and its volume/bed mass ratio is low.

To study the effect of the pyrolysis pressure on product characteristics, pyrolysis runs have been conducted under 1 and 0.25 atm at 400 and 500 °C. The runs have been carried out in continuous mode by feeding 2 g min^{-1} of biomass. The bed was made up of 100 g of sand (particle size of 0.3−0.63 mm), guaranteeing a good heat transfer and isothermicity. The CSBR is characterized by the vigorous solid circulation, resulting in no significant temperature gradients in the bed, as previously proven in a pilot plant unit.[34] Furthermore, heat transfer toward the biomass particle mainly occurs by sand-based conduction in the annulus zone, but convection also plays a significant role in the spout region because of the high gas flow rate. Most of the solid is descending in the annulus at the same time as there is solid cross-flow from the annulus into the spout (perfect mixing assumed). On the other hand, the

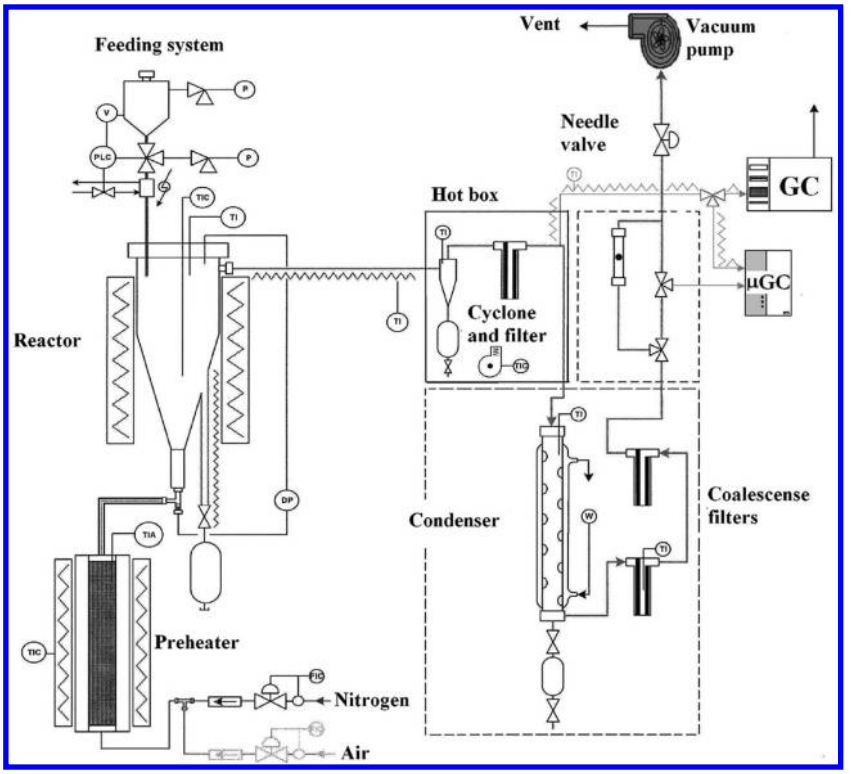

Figure 1. Schematic diagram of the pyrolysis pilot plant.

main fraction of the gas crosses the spout in plug flow and a lower fraction circulates across the annular zone, where the flow is considered dispersed plug flow.[33]

In a previous paper,[50] a hydrodynamic study was carried out under vacuum and at high temperatures (up to 600 °C), and it was concluded that the minimum spouting velocity under these conditions slightly increases when the operating pressure is reduced. However, this effect because of the lower density of the gas under vacuum conditions attenuates as the temperature is increased, which partially offsets the increase in the N_2 mass flow rate required for the spouting regime. In this study, the nitrogen gas flow rate is 1.2 times that corresponding to the minimum spouting velocity, 11.5 and 3.2 NL min^{-1} at 400 °C and 10.5 and 3 NL min^{-1} at 500 °C, under 1 and 0.25 atm, respectively. These values have been experimentally established as adequate for bed stability and practically coincide with those calculated by means of the correlation proposed to account for temperature and pressure effects on minimum spouting velocity.[50]

2.4. Product Analysis. Product analysis has been carried out online by analyzing the reactor outlet stream by means of a gas chromatograph (Varian 3900) equipped with a flame ionization detector (FID). To avoid the condensation of heavy oxygenated compounds, the line from the reactor outlet to the chromatograph is heated to a temperature of 280 °C and, in addition, the reactor outlet stream has been diluted with an inert gas. A calibration has been performed to obtain the response factors of the FID device to oxygenated compounds. Note that, unlike hydrocarbons, the FID response to oxygenated compounds is not proportional to their mass. Furthermore, noncondensable products leaving the condensation system have been monitored using a microgas chromatograph (GC, Varian 4900). This micro-GC has also been used to measure the water yield, following a similar procedure to that described for the standard GC.

Given that the unit described in Figure 1 needs to be fully airtight for operating under vacuum, a leak test has been carried out before each pyrolysis run to ensure no air is entering the reaction medium. In each run, 100 g of biomass has been continuously fed and samples have been taken after operating for at least 10 min under the same conditions. Each run has been repeated several times to ensure the reproducibility of the process. The experimental error is low for most of the compounds, around 1%; however, certain products are under higher uncertainty, with the error being lower than 5% in these cases. The mass balance is closed using the information obtained by weighing the char collected by the lateral outlet and at the cyclone and reactor at the end of the continuous run and the online chromatographic analysis. To validate the mass balance, an internal standard (cyclohexane) has been introduced in some of the experiments through an inlet located in the heated line running from the reactor to the chromatograph, which allowed for the obtainment of 94% mass balance closure. A more detailed description of the procedure can be found elsewhere.[54,55]

The identification of the liquid products has been performed in a gas chromatograph/mass spectrometer (GC/MS, Shimadzu UP-2010S), and the gaseous products have also been analyzed by means of a micro-GC connected to a MS (Agilent 5975B). The fuel properties of the bio-oil have been measured by carrying out an ultimate analysis and measuring the calorific value and water content (ASTM D95 standard). The surface area and pore volume of the char have been determined from nitrogen adsorption−desorption isotherms obtained in a Micromeritics ASAP 2000. The surface characteristics of the chars have been analyzed using a JEOL JSM-6400 scanning electronic microscope (SEM).

3. RESULTS

3.1. Kinetic Study in Thermobalance. Figure 3 shows the evolution of conversion (graph a) and differential thermogravimetry (DTG) curve (graph b) with the temperature for the two levels of pressure studied. As observed, the influence of vacuum operation on the kinetics of biomass pyrolysis is negligible,

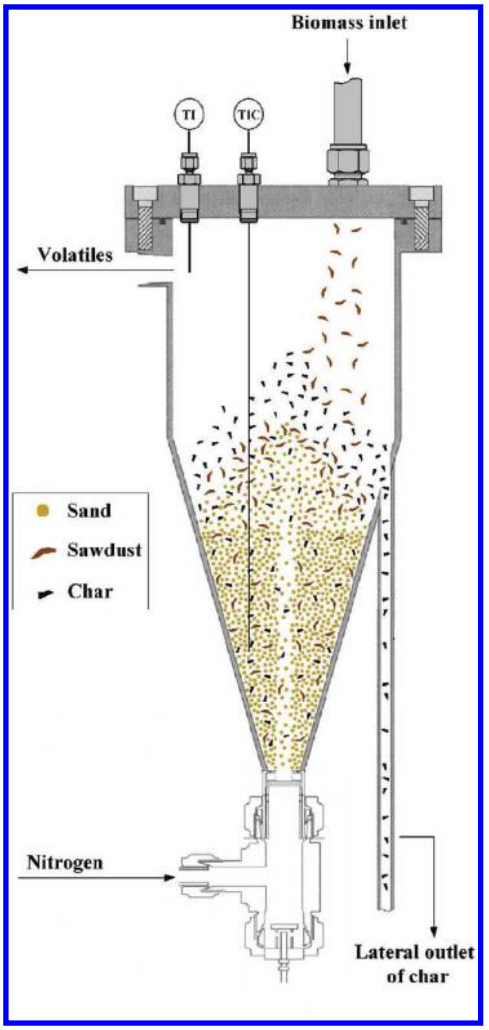

Figure 2. Schematic diagram of the CSBR in the continuous pyrolysis process.

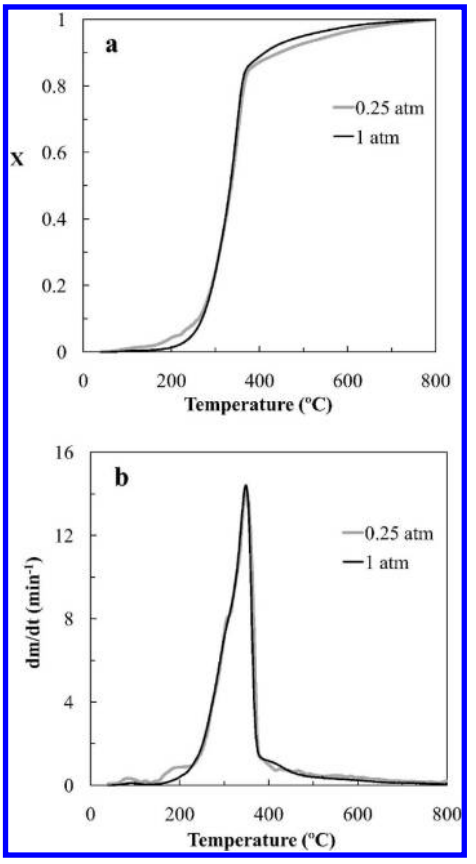

Figure 3. (a) Evolution of conversion and (b) DTG curve with the temperature under atmospheric pressure and vacuum.

because only a slight difference is appreciated between 130 and 220 °C, corresponding to extractive volatilization.[58] This effect of vacuum differs from that observed for tire pyrolysis, where vacuum had a positive effect on pyrolysis kinetics.[47] This difference is explained by the structure of tire particles, given that vacuum enhances volatilization and diffusion within the particle. The biomass particle is initially more porous than the tire one; therefore, the diffusion within the particle will not be improved to the same extent, resulting in a reduced influence of vacuum on the pyrolysis kinetics. However, mass evolution with the temperature (figures are not shown) reveals that vacuum has a great influence on the char fraction; i.e., its yield is around 23% under 1 atm and 18% under 0.25 atm, at the end of the experiments (800 °C).

Biomass has three main elements: hemicellulose, cellulose, and lignin, which, in the case of pinewood sawdust, account approximately for 23, 51, and 26 wt %, respectively,[24,25,59,60] and lower amounts of extractives and ash. As shown in Figure 3b, biomass pyrolysis occurs in a wide temperature range, resulting in a wide band that peaks at 350 °C, in which the decomposition of the three biomass components overlaps. Biomass pyrolysis kinetics has been extensively studied in the literature. White et al.[61] carried out a critical review of kinetic models and mathematical approximations currently employed, emphasizing that the thermal decomposition of biomass proceeds via a very complex set of competitive and concurrent reactions. In addition, different factors can influence the kinetic parameters, including process conditions, heat- and mass-transfer limitations, physical and chemical heterogeneity of the sample, and systematic errors.

With the aim of simplifying the kinetic study, a large number of authors consider that the pyrolysis process is the sum of three independent and parallel reactions corresponding to the decomposition of hemicellulose, cellulose, and lignin, which takes place at 200−350, 280−350, and 180−600 °C, respectively.[58,62−67] Most kinetic studies are performed in thermogravimetric devices, although heating rates, gas residence times, and process temperatures are different from those in typical flash pyrolysis reactors. In fact, these thermogravimetric studies are widely accepted because they allow for ascertaining fuel reactivity at kinetic control conditions, which can be further used in more complex mechanisms that also take into account transport phenomena inside the biomass particle during pyrolysis under fast heating rates and low residence times.[68]

The kinetic study of pinewood sawdust pyrolysis has been carried out only for the atmospheric process, considering three independent parallel reactions, corresponding to the devolatilization of hemicellulose, cellulose, and lignin. The analysis of the kinetic data has been carried out by deconvolution of the DTG curve and numerically solving the conservation equations and calculating the kinetic parameters of best fit.

The overall kinetic equation is

$$\left(-\frac{1}{W_0}\right)\left(\frac{dW}{dt}\right) = \sum_{i=1}^{3} c_i k_i \left[\frac{(W_i - W_{\infty,i})}{(W_{0,i} - W_{\infty,i})}\right]^{n_i} \quad (1)$$

Considering the following definition of conversion

$$X = \frac{W_0 - W}{W_0 - W_\infty} \quad (2)$$

and assuming a first-order kinetics for each component, eq 1 can be expressed as

$$\frac{dX}{dt} = c_1 k_1 (X_{\infty,1} - X_1) + c_2 k_2 (X_{\infty,2} - X_2) + c_3 k_3 (X_{\infty,3} - X_3) \quad (3)$$

where X_i and $X_{\infty,i}$ are the conversion at t time and the final conversion of each component, respectively (defined according to eq 2), and c_i is the mass concentration of hemicellulose, cellulose, and lignin, whose values are 0.23, 0.51, and 0.26, respectively.[24,25,59,60]

Given that the runs are carried out following a temperature ramp, the Arrhenius equation is considered in the kinetic constants in eq 3. The calculation of the kinetic parameters, frequency factor, $(k_0)_i$, and activation energy, E_i, has been carried out by fitting the experimental results obtained by deconvolution to eq 3 integrated for each component. From the experimental TG curve and following a second-order approximation with central derivatives, the theoretical DTG curve is obtained by minimizing the error objective function

$$\mathrm{EOF} = \frac{\sum_{j=1}^{L} [(\mathrm{DTG})_{\mathrm{calculated}} - (\mathrm{DTG})_{\mathrm{experimental}}]^2}{L} \quad (4)$$

where L is the number of the available experimental data.

The fit between the calculated results and the experimental values of X_i is carried out by means of a program written in MATLAB using the subroutine fminsearch with the Levenberg−Marquardt algorithm to minimize the error objective function (eq 4) and the subroutine ode45 based on the Runge−Kutta−Fehlberg pair of orders 4 and 5 for solving the differential equations for each component in the sample (eq 3).

Figure 4 compares the experimental results (points) and those calculated (thick line) for the evolution with the temperature of the overall conversion (graph a) and DTG curve (graph b). The fit between the experimental and calculated results is satisfactory, although there is a slight difference at the beginning of the devolatilization, because the small fraction of extractives has not been considered in the kinetic model.

Table 2 shows the results obtained for the frequency factor and activation energy for the three components. The kinetic parameters are similar to those obtained by other authors, who also carried out the kinetic study considering three parallel reactions corresponding to hemicellulose, cellulose, and lignin. Thus, the value ranges for the activation energy are 105−115 kJ mol^{-1} for hemicellulose, 195−215 kJ mol^{-1} for cellulose, and 35−65 kJ mol^{-1} for lignin.[58,64,67,69]

The results obtained by Gronli et al.[58] for pinewood are very similar to those obtained in this work. Thus, the values reported by these authors for the activation energies are 100, 236, and 46 kJ mol^{-1} for the hemicellulose, cellulose, and lignin, respectively,

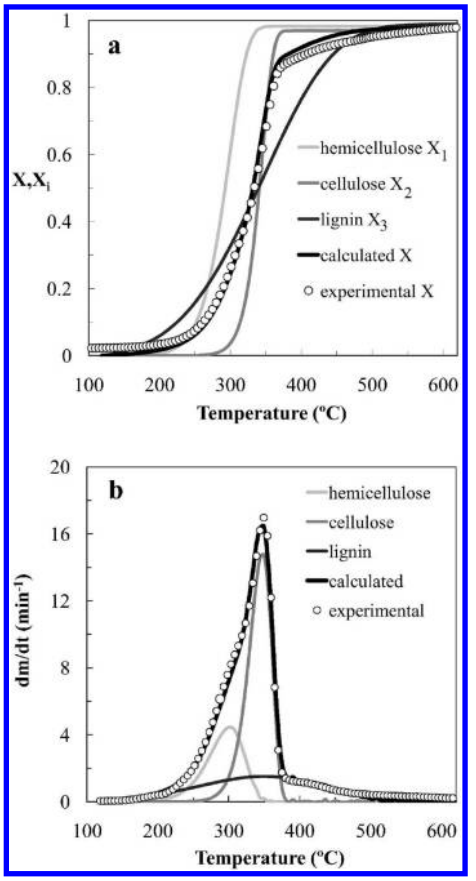

Figure 4. Comparison of experimental results (points) and those estimated using the kinetic model (thick line) for the (a) evolution of sample conversion with temperature and (b) DTG curve.

Table 2. Values of Frequency Factor, $(k_0)_i$, and Activation Energy, E_i, for the Pyrolysis of the Three Biomass Components, with a 95% Confidence Interval

component	log $(k_0)_i$ (s^{-1})	E_i (kJ mol^{-1})
hemicellulose	8.14	115 ± 9
cellulose	15.96	218 ± 15
lignin	0.25	35 ± 2

and the values for the logarithm of the frequency factor, log k_0, are 6.3, 17.3, and 0.5 s^{-1}, respectively. Varhegyi et al.[69] calculated the parameters corresponding to the hemicellulose and cellulose fractions of beech based on the kinetic parameters obtained by Gronli et al.[58] for lignin. Their values for activation energy are 97 and 234 kJ mol^{-1}, and those for the logarithm of the frequency factor, log k_0, are 6.4 and 17.4 s^{-1}, respectively. Branca et al.[67] used beechwood with very high heating rates (108 K min^{-1}), and their values for activation energy are 147, 193, and 181 kJ mol^{-1} for hemicellulose, cellulose, and lignin, respectively. Other authors[66,70] studied the kinetics of rice husk pyrolysis by means of the linearization of the kinetic equations, and the values for activation energy are 154, 199, and 34 kJ mol^{-1}, respectively.

3.2. Continuous Vacuum Flash Pyrolysis in the Bench-Scale Conical Spouted Bed Unit. As mentioned above, the aim of vacuum operation is to obtain operational advantages related to the reduction in the N_2 mass flow rate and improving the

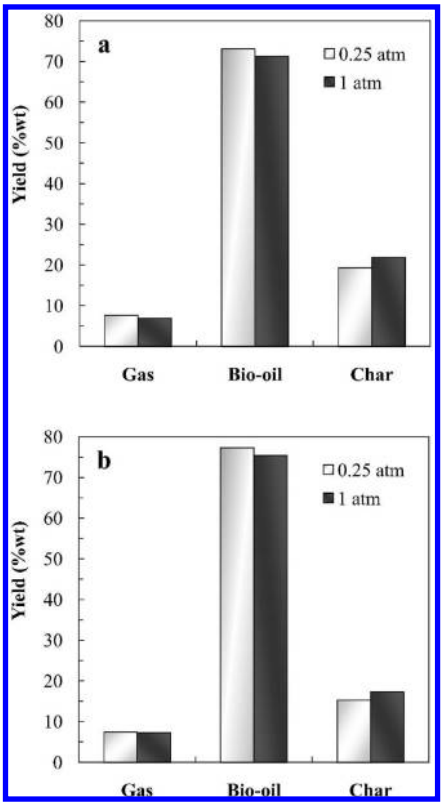

Figure 5. Effect of the pressure on the yields of the different product fractions, at (a) 400 °C and (b) 500 °C.

condensation of the volatile products, which means energy saving. Thus, the adiabatic theoretical power has been calculated using the equation corresponding to vacuum pumps and considering to an efficiency of 60%,[71] showing that the energy required to operate under 1 atm is higher than that required to operate under a mild vacuum (0.25 atm). The power needed to heat the gas flow rate corresponding to 1 atm is 103 W, whereas that corresponding to 0.25 atm is only 30 W, with vacuum generation requiring 55 W. Furthermore, the energy recovered by cooling the outlet stream is a low-level thermal energy and, consequently, difficult to integrate in the overall process. Accordingly, the energy saving associated with the condensation of a smaller outlet stream should also be taken into account. However, these advantages will only apply if this reduction in the inert flow rate does not compromise the yield and composition of the bio-oil obtained.

Furthermore, vacuum operation in a CSBR requires a slight increase in the volumetric flow rate of N_2 (approximately 5% for 0.25 atm between 400 and 500 °C), in comparison to the pyrolysis at atmospheric pressure,[50] with the resulting decrease in the average residence time of the volatiles in the reactor in the same proportion. Pyrolysis results would be affected as a consequence of this change, given that the reactor performance is significantly affected by the hydrodynamic behavior of the conical spouted bed.

3.2.1. Product Yields. The pyrolysis of pinewood sawdust has been studied at 400 and 500 °C, and the effect of the pressure has been studied under atmospheric pressure and vacuum (0.25 atm). The products have been grouped into three different fractions: gas fraction, bio-oil, and char. All of the results are expressed on a raw biomass basis. Figure 5 shows the evolution of the lumps obtained under the different conditions studied at 400 °C (graph a) and at 500 °C (graph b). The temperature values correspond to the range where the bio-oil yield is maximized in a CSBR and other technologies for biomass flash pyrolysis.[2,11,12] Furthermore, the vacuum level of 0.25 atm can be considered to be a limit value from the point of view of the large-scale implementation of the process under vacuum, because a more severe vacuum involves a remarkable increase in the cost of the equipment.

As observed, pressure reduction results in a slight increase in the yields of the gas and bio-oil fractions and a decrease in the char yield. The gas yield accounts for 7−8 wt % at both temperatures studied. However, the yield of bio-oil increases from 70 wt % under 1 atm to 72 wt % under 0.25 atm when the pyrolysis temperature is 400 °C, and this increase is from 75 to 77 wt % at 500 °C. With regard to the char yield, there is a decrease of 2 wt % at both temperatures, i.e., a yield of 19 wt % at 400 °C and 15 wt % at 500 °C, respectively. This decrease in the char yield has already been reported in the thermogravimetric experiments, although the yields in this case are higher because of the lower heating rate and higher gas residence time.

The effect of vacuum is explained by the fact it enhances the desorption and diffusion of the volatiles formed within the porous structure of the biomass particle toward the outside, which is due to the positive pressure gradient generated by vacuum for that flow. The faster diffusion of the volatiles reduces their residence time inside the particle and, consequently, limits secondary and cracking reactions, increasing the yield of bio-oil. The results of char yield reduction, 2 wt % at both temperatures, emphasize the significance of the limitation in the formation of carbonaceous additives on the char by means of polycondensation/polymerization reactions from volatile compounds.[36]

Furthermore, the effect of the temperature when operating under vacuum conditions is similar to when operating under atmospheric pressure, resulting in an increase in the yield of bio-oil and a decrease in the char yield when the temperature is raised from 400 to 500 °C, as reported in previous papers.[29,30]

The results obtained by the research group of Laval University by carrying out the pyrolysis reactions in a moving bed reactor suggest that the secondary cracking reactions are more significant in their type of reactor than in the conical spouted bed. They performed continuous pyrolysis under vacuum (between 0.007 and 0.4 atm) of bark mixtures of several trees (spruce, birch, etc.) at 500 °C and obtained approximately 12−28 wt % gas, 45−63 wt % bio-oil, and 22−28 wt % char.[40,41,43−45]

Furthermore, Murwanashyaka et al.[40,41] reported that, when the operating pressure decreased from 0.4 to 0.007 atm, the bio-oil yield increased by 10 wt %, to a value of 63 wt %. Moreover, Darmstadt et al.[37] and Boucher et al.[38,39] operated also under vacuum and studied the influence of the feeding mode of the raw material. They concluded that, when operation is performed by feeding the biomass discontinuously, the char yield is higher and, therefore, that of bio-oil is lower. Other authors, operating with fixed beds under vacuum, obtained a lower yield of bio-oil (between 50 and 60 wt %), by feeding either pinewood[72] or other biomass feedstocks.[73]

3.2.2. Gas Fraction. Table 3 shows the yields of the compounds in the gaseous fraction for sawdust pyrolysis under 0.25 and 1 atm. Gas is made up mainly of carbon dioxide and carbon monoxide and lower amounts of C_1−C_4 hydrocarbons. Vacuum operation has a significant influence on the carbon dioxide yield, given that it increases at both pyrolysis temperatures when the

Table 3. Comparison of the Yields (wt %) of Gaseous Products Obtained under Atmospheric Pressure and Vacuum at 400 and 500 °C

	400 °C		500 °C	
compound	0.25 atm	1 atm	0.25 atm	1 atm
CO_2	5.08	4.36	3.47	3.27
CO	2.49	2.42	3.34	3.38
H_2	0.01		0.01	0.00
CH_4	0.06	0.05	0.32	0.36
ethylene	0.02	0.01	0.10	0.09
ethane	0.01	0.01	0.04	0.06
propylene	0.02	0.01	0.11	0.07
propane	0.01	0.01	0.02	0.05
2-methyl-1-propene	0.00	0.01	0.04	0.02
2-butene			0.03	0.01
unidentified		0.00	0.04	0.01
gas	7.69	6.87	7.51	7.33

pressure is decreased, with this effect being more pronounced at 400 °C. However, carbon monoxide and C_1-C_4 hydrocarbon yields remain practically constant. The effect of the temperature is similar in both atmospheric and vacuum processes, as the CO_2 yield decreases as the temperature is increased, whereas those of CO and C_1-C_4 hydrocarbons increase. This is mainly because most CO_2 is produced by carboxyl release at relatively low temperatures, but CO and CH_4 are produced at higher temperatures instead of CO_2 because of the secondary cracking of volatiles.[12,74]

3.2.3. Bio-oil Composition and Properties. Bio-oil is a very complex mixture of oxygenated compounds; therefore, to simplify the results, the products have been lumped according to their functional groups. Table 4 shows the yields of the functional groups and some of the main products.

The main product in the bio-oil is water, whose yield is around 23 wt % at 400 °C and 25 wt % at 500 °C. Under vacuum there is a slight decrease in the water yield, because of the reduction in the secondary cracking reactions.

Phenols are the prevailing organic functional group in the bio-oil, and their yield increases when operating under vacuum. This group has in turn been divided into three lumps: catechols (benzenediols), guaiacols (methoxyphenols), and alkyl-phenols. Ba et al.[44] found that, in the vacuum pyrolysis of different bark mixtures (spruce and fir), the bio-oil was composed mostly of phenols, with guaiacols and catechols as the main products. García-Pérez et al.[42] carried out sugar cane vacuum pyrolysis, and in addition to phenols, they identified several compounds, such as acids, ketones, aldehydes, furans, levoglucosan, etc.

As observed in Table 4, pressure affects differently at 400 and 500 °C. Whereas at 400 °C, the yields of guaiacols and alkyphenols increase when operating under vacuum, the catechol yield increases significantly at 500 °C, mainly because of the rise of the 4-methyl catechol yield. On the other hand, the temperature has a great influence in the composition of the phenolic group, because guaiacols are the main compounds at the lower temperature, whereas the catechol yield increases at the higher temperature. Murwanashyaka et al.[40,41] identified similar phenolic compounds by operating in a moving bed reactor at 25−550 °C and 0.007 atm. Similarly, they observed that guaiacols and syringols were the main compounds at low temperatures, but the methoxy groups of these compounds were transformed into catechols at higher temperatures.

Table 4. Comparison between the Yields (wt %) of the Functional Groups and the Main Individual Components in the Bio-oils Obtained under Atmospheric Pressure and Vacuum at 400 and 500 °C

	400 °C		500 °C	
compound	0.25 atm	1 atm	0.25 atm	1 atm
acids	3.32	2.49	2.40	2.73
formic acid	0.20	0.11	0.16	0.17
acetic acid	0.74	0.44	0.74	1.11
acetic anhydride	1.06	0.93	0.46	0.90
dimethylbenzoic acids	0.33	0.37	0.49	0.26
aldehydes	2.41	2.44	2.37	1.93
formaldehyde	0.36	0.26	0.03	0.35
acetaldehyde	0.05	0.06	0.22	0.16
2-propenal	0.00	0.02	0.15	0.12
benzaldehydes	0.77	1.30	0.93	0.49
alcohols	2.26	1.75	1.56	2.00
methanol	0.72	0.52	0.64	0.69
glycerin	1.41	1.14	0.73	1.11
ketones	6.79	5.87	5.81	6.37
acetone	0.87	0.51	0.74	0.67
acetol	1.00	1.38	0.69	1.53
cyclopentanediones	0.77	0.74	0.58	0.52
cyclohexanone	1.14	1.34	0.56	1.23
hydroxymethoxyphenyl ketones	1.59	0.59	1.54	1.09
phenols	16.35	15.57	18.75	16.49
alkyl phenols	3.04	2.12	1.18	1.80
phenol	0.13	0.22	0.14	0.40
cresols	1.88	0.99	0.22	0.67
catechols	2.94	3.15	10.09	7.16
catechol	1.26	1.66	4.20	4.08
methyl catechols	0.45	0.64	4.46	2.40
guaiacols	10.37	9.94	7.48	7.53
guaiacol	3.14	4.12	0.65	1.86
eugenol	2.94	2.50	1.51	1.40
furans	2.58	3.30	1.63	3.32
furan	0.13	0.84	0.17	0.71
2-furanmethanol	1.18	1.05	0.33	0.75
2,3-dibenzofuran	0.77	0.91	1.00	0.61
saccharides	3.55	5.26	6.26	4.46
3,4-altrosan	2.07	0.09	0.00	0.00
2,3-anhydro-D-mannosan	3.24	2.67	1.39	1.56
levoglucosan	0.22	0.52	3.27	2.78
others	0.14	0.09	0.03	0.06
unidentified	11.95	10.70	13.41	12.61
water	23.00	23.33	24.98	25.36
bio-oil	73.01	71.23	75.33	77.19

Ketones are one of the significant functional groups, and the effect of the pressure on their yield reverses from one temperature studied to the other. At 400 °C, the ketone yield increases under vacuum because of the increase in the heaviest compounds, whereas at 500 °C, it decreases, as their cracking is enhanced.

Table 5. Pressure Effect on Bio-oil Properties

	400 °C		500 °C	
properties	0.25 atm	1 atm	0.25 atm	1 atm
Ultimate Analysis (wt %)				
carbon	43.9	42.7	42.9	41.7
hydrogen	8.1	8.1	8.0	8.1
nitrogen	0.1	0.1	0.2	0.2
oxygen	47.9	49.1	48.9	50.0
water content (wt %)	34.5	35.8	35.3	36.7
HHV (MJ kg^{-1})	15.8	15.2	15.4	14.6

At 400 °C, the yield of saccharides decreases by lowering pressure, but at 500 °C, the reverse is true. The reduction at 400 °C stems from the dramatic decrease in 3,4-altrosan and levoglucosan under vacuum operation. Nevertheless, at 500 °C (the temperature at which the levoglucosan yield is maximized under atmospheric pyrolysis),[30] there is a 1 wt % increase in the yield of levoglucosan. This result is due to the lower cracking of levoglucosan under vacuum conditions. A similar effect has been reported in the literature when the residence time of volatiles is decreased.[75]

In addition, the yield of furans decreases when the operating pressure is decreased, mainly because of the reduction in the furan yield. Acids follow a different trend depending upon the pyrolysis temperature. At 400 °C, their yield increases under subatmospheric pressure, whereas at 500 °C, it decreases, which is due to the changes in the yield of acetic acid.

The aldehyde yield remains almost constant at 400 °C but increases when operating under vacuum conditions at 500 °C because of the increase in the benzaldehyde yield. The yield of alcohols at 400 °C slightly increases under low pressures, but at 500 °C, the reverse is true.

As mentioned above, vacuum operation reduces secondary cracking reactions. Consequently, the bio-oil obtained is composed of heavier compounds with a higher molecular weight. This effect is more pronounced at 500 °C because of the increase in catechols, saccharides, heavy ketones, and benzaldehydes. The same effect has been observed in a previous study on the pyrolysis of waste tires, in which the yield of the C_{11+} (tar) fraction increased under vacuum operation and, consequently, a heavier liquid fraction was obtained, which is suitable for use as diesel fuel.[46]

Bio-oil has been characterized to evaluate its fuel properties, by means of ultimate analysis and measuring its water content and calorific value (on a wet basis) (Table 5).

As observed, bio-oil is highly oxygenated, although a small increase in the carbon content can be noticed under subatmospheric pressure, which is due to the increase in the yield of heavier and less oxygenated compounds. Furthermore, the water yield also decreases slightly, contributing to a decrease in the oxygen content. Therefore, the calorific value of the bio-oils obtained under vacuum pressure is higher, slightly improving valorization prospects of bio-oil as fuel. In a previous paper,[30] other properties of the bio-oil obtained under atmospheric pressure have been analyzed, such as pH, density, and viscosity, concluding that the values are similar to those obtained in more conventional reactors.

3.2.4. Char Characterization. Char has also been characterized (Table 6), given that it may have an application as an active carbon after being subjected to an activation process.[14] Similar carbon content values have been obtained by other authors studying vacuum biomass pyrolysis.[37,42,76,77]

Table 6. Influence of the Pyrolysis Pressure on Char Properties

	400 °C		500 °C	
	0.25 atm	1 atm	0.25 atm	1 atm
Ultimate Analysis (wt %)				
carbon	79.7	75.0	84.5	85.2
hydrogen	3.4	3.8	2.8	3.0
nitrogen	0.01	0.2	0.1	0.1
oxygen	16.9	21.0	12.6	11.8
Proximate Analysis (wt %)				
volatile matter	27.6	37.6	24.0	23.5
fixed carbon	69.8	60.2	72.8	73.6
ash	2.6	2.2	3.2	2.9
HHV (MJ kg^{-1})	26.8	21.6	28.2	30.4
Surface Characteristics				
BET surface (m^2 g^{-1})	5.1	1.9	79.2	16.2
average pore diameter (Å)	464.3	472.1	53.2	453.5

The results shown in Table 6 show that temperature has a positive influence on the carbon and fixed-carbon content of the char but the pressure effect is not so clear. At 400 °C, vacuum enhances the carbon content, whereas at 500 °C, there is no noticeable change and the carbon yield decreases slightly at low pressure.

Furthermore, vacuum improves the surface properties of the char, as the BET surface area increases and average pore diameter reduces because of the minimization of secondary reactions of repolymerization and carbonization and the resulting reduction in char pore blockage. This effect is more pronounced at 500 °C, as the temperature enhances these advantages. It is noteworthy that the char obtained at 500 °C and under 0.25 atm has two prevailing pore sizes: mesopores of 100 Å and micropores of 19 Å.

Figure 6 shows the SEM images of the raw biomass (graph a) and chars obtained at 500 °C under 0.25 atm (graph b) and 1 atm (graph c). These images confirm the amorphous structure of the char. The char longitudinal surface structure is formed by grooves, which are worse defined in the case of the raw biomass, with the surface being flatter. The char obtained under 1 atm does not have well-defined grooves, whereas that obtained under 0.25 atm has more and deeper grooves that give rise to a rough appearance with smaller pores.

These surface properties suggest that the char obtained under vacuum is an interesting raw material for its further valorization to obtain active carbon by means of activation processes with steam, CO_2, or solvents. Thus, several authors have obtained active carbons with BET surface areas in the 1000−1800 m^2 g^{-1} range from biomass chars.[72,76−78] The active carbons obtained from biomass can be used in the adsorption of pollutants,[15] as catalyst supports,[16,17] and as acid catalysts.[18,19]

4. CONCLUSION

The CSBR has proven to be a suitable technology to perform vacuum biomass flash pyrolysis, obtaining high bio-oil yields, up to 77 wt % at 500 °C. Vacuum is interesting for increasing process

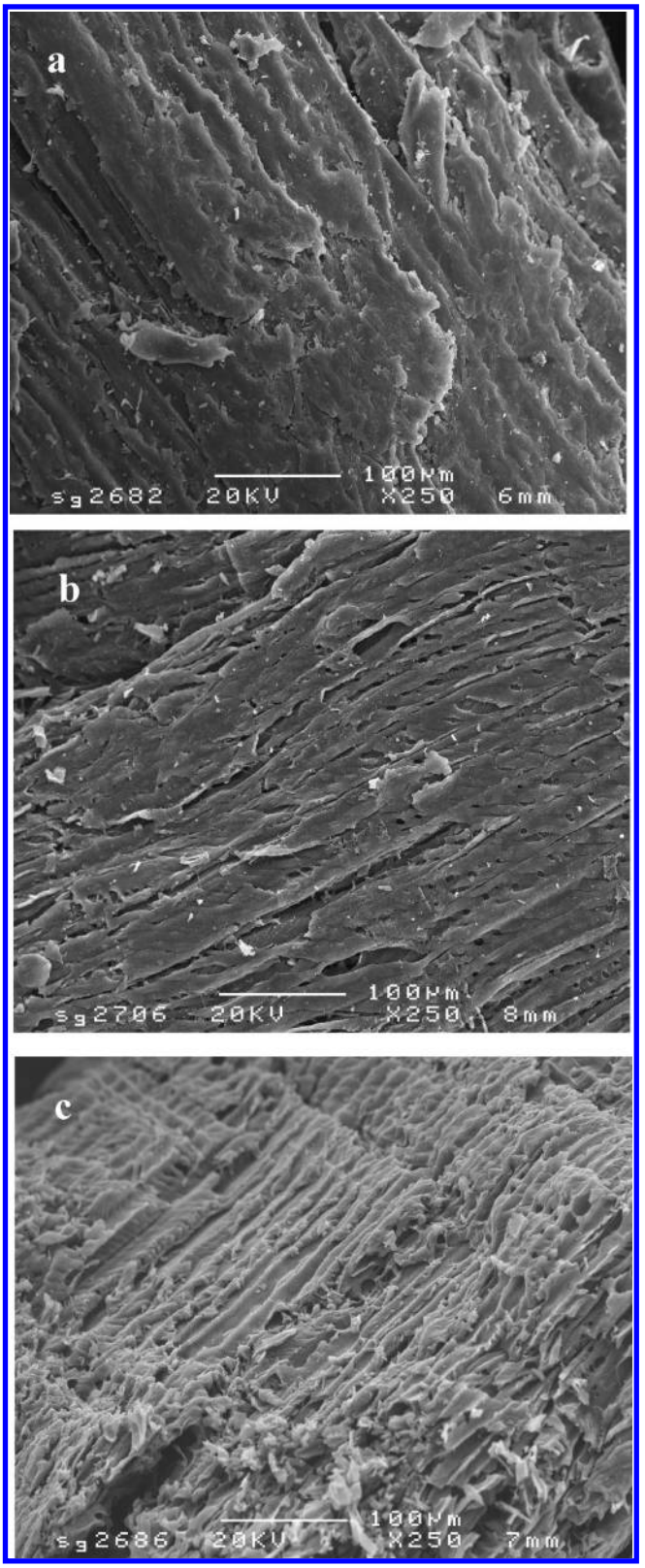

Figure 6. SEM photomicrographs of (a) biomass and chars obtained at 500 °C and (b) 0.25 atm and (c) 1 atm.

viability, because the nitrogen mass flow rate is lower. Consequently, less energy is required to heat this carrier gas, and moreover, the condensation of the product stream is easier. Furthermore, the low reactor volume/bed mass ratio in a CSBR allows for the performance of vacuum operation in the biomass pyrolysis process.

Vacuum down to 0.25 atm does not affect the kinetics of biomass pyrolysis, except for the first stage of the process related to the volatilization of the extractives. The kinetics follows a model with three parallel and independent reactions, corresponding to the decomposition of hemicellulose, cellulose, and lignin, and the kinetic parameters calculated are similar to those obtained with other technologies for biomass pyrolysis.

Vacuum has a low influence on the yields of the different fractions, although there is a slight increase in the bio-oil yield when operating under vacuum. The influence is more significant regarding product characteristics and their composition. The main advantages of vacuum operation over atmospheric operation are a less oxygenated bio-oil and a char fraction with improved surface characteristics, which gives way to an active carbon of higher quality after subjecting it to activation processes. Vacuum slightly increases the yields of heavier compounds in the bio-oil, such as phenols and levoglucosan, and given that the water yield is slightly reduced, the calorific value of bio-oil is improved.

AUTHOR INFORMATION

Corresponding Author

*Telephone: +34946012527. Fax: +34946013500. E-mail: martin.olazar@ehu.es.

ACKNOWLEDGMENT

This research was carried out with the financial support of the Ministry of Science and Education of the Spanish Government (Project CTQ2007-61167) and the University of the Basque Country (Project GICO7/24-IT-220-07).

NOMENCLATURE

c_i = mass concentration of the ith component
DTG = differential thermogravimetry
E_i = activation energy of the ith component (kJ mol^{-1})
$(k_0)_i$ = frequency factor of the ith component (s^{-1})
k_i = kinetic constant for the weight loss of each i component (s^{-1})
L = number of experimental data available
n = reaction order
t = time (s)
W, W_0, and W_∞ = weight of the biomass sample at t time, at the beginning of pyrolysis, and at the end of pyrolysis, respectively (mg)
W_i, $W_{0,i}$, and $W_{\infty,i}$ = weight of the ith component in the sample at t time, at the beginning, and at the end, respectively (mg)
X = conversion of the biomass sample by mass unit of pyrolysable mass
X_i and $X_{\infty,i}$ = conversion of the ith component at t time and at the end, respectively

REFERENCES

(1) Czernik, S.; Bridgwater, A. *Energy Fuels* **2004**, *18*, 590–598.
(2) Bridgwater, A. V. *Biomass Bioenergy* **2011**, DOI: 10.1016/j.biombioe.2011.01.048.
(3) Stöcker, M. *Angew. Chem., Int. Ed.* **2008**, *48*, 9200–9211.

(4) Sandun, F.; Adhikari, S.; Chauda, C.; Naveen, M. *Energy Fuels* **2006**, *20*, 1727–1737.
(5) Huber, G.; Corma, A. *Angew. Chem., Int. Ed.* **2007**, *46*, 7184–7201.
(6) Demirbas, A. *Energy Convers. Manage.* **2009**, *50*, 2239–2249.
(7) Corma, A.; Huber, H.; Sauvanaud, L.; O'Connor, P. *J. Catal.* **2007**, *247*, 307–327.
(8) Graça, I.; Fernández, A.; Lopes, J. M.; Ribeiro, M. F.; Laforge, S.; Magnoux, P.; Ramôa Ribeiro, F. *Fuel* **2011**, *90*, 467–476.
(9) Bertero, M.; de la Puente, G.; Sedran, U. *Energy Fuels* **2011**, *25*, 1267–1275.
(10) Gayubo, A. G.; Valle, B.; Aguayo, A. T.; Olazar, M.; Bilbao, J. *Ind. Eng. Chem. Res.* **2010**, *49*, 123–131.
(11) Mohan, D.; Pittman, C.; Steele, P. *Energy Fuels* **2006**, *20*, 848–889.
(12) Neves, D.; Thunman, H.; Matos, A.; Tarelho, L.; Gómez-Barea, A. *Prog. Energy Combust. Sci.* **2011**, *37*, 611–630.
(13) Bridgwater, A.; Meier, D.; Radlein, D. *Org. Geochem.* **1999**, *30*, 1479–1493.
(14) Ioannidou, O.; Zabaniotou, A. *Renewable Sustainable Energy Rev.* **2007**, *11*, 1966–2005.
(15) Palomar, J.; Lemus, J.; Gilarranz, M. A.; Rodríguez, J. J. *Carbon* **2009**, *47*, 1846–1856.
(16) Calvo, I.; Gilarranz, M. A.; Casas, J. A.; Mohedano, A. F.; Rodriguez, J. J. *Chem. Eng. J.* **2010**, *163*, 212–218.
(17) de Pedro, Z. M.; Casas, J. A.; Gómez-Sainero, L. M.; Rodríguez, J. J. *Appl. Catal., B* **2010**, *98*, 79–85.
(18) Bedia, J.; Rosas, J. M.; Vera, D.; Rodríguez-Mirasol, J.; Cordero, T. *Catal. Today* **2010**, *158*, 89–96.
(19) Bedia, J.; Barrionuevo, R.; Rodriguez-Mirasol, J.; Cordero, T. *Appl. Catal., B* **2011**, *103*, 302–210.
(20) Jha, P.; Biswas, A. K.; Lakaria, B. L.; Rao, S. A. *Curr. Sci.* **2010**, *99*, 1218–1225.
(21) Boateng, A.; Daugaard, D.; Goldberg, N.; Hicks, K. *Ind. Eng. Chem. Res.* **2007**, *46*, 1891–1897.
(22) Garcia-Perez, M.; Wang, X.; Shen, J.; Rhodes, M.; Tian, F.; Lee, W.; Wu, H.; Li, C. *Ind. Eng. Chem. Res.* **2008**, *47*, 1846–1854.
(23) Heo, H. S.; Park, H. J.; Park, Y. K.; Ryu, C.; Suh, D. J.; Suh, Y. W.; Yim, J. H.; Kim, S. S. *Bioresour. Technol.* **2010**, *101*, 1–6.
(24) Oasmaa, A.; Kuoppala, E.; Solantausta, Y. *Energy Fuels* **2003**, *17*, 433–443.
(25) Oasmaa, A.; Solantausta, Y.; Arpiainen, V.; Kuoppala, E.; Sipila, K. *Energy Fuels* **2010**, *24*, 1380–1388.
(26) Léde, J.; Broust, F.; Ndiaye, F. T.; Ferrer, M. *Fuel* **2007**, *86*, 1800–1810.
(27) Ingram, L.; Mohan, D.; Bricka, M.; Steele, P.; Strobel, D.; Crocker, D.; Mitchell, B.; Mohammad, J.; Cantrell, K.; Pittman, C. *Energy Fuels* **2008**, *22*, 614–625.
(28) Das, P.; Sreelatha, T.; Ganesh, A. *Biomass Bioenergy* **2004**, *27*, 265–275.
(29) Aguado, R.; Olazar, M.; San Jose, M. J.; Aguirre, G.; Bilbao, J. *Ind. Eng. Chem. Res.* **2000**, *39*, 1925–1933.
(30) Amutio, M.; Lopez, G.; Artetxe, M.; Elordi, G.; Olazar, M.; Bilbao, J. *Resour., Conserv. Recycl.* **2011**, DOI: 10.1016/j.resconrec.2011.04.002.
(31) Olazar, M.; San José, M. J.; Peñas, F. J.; Aguayo, A. T.; Bilbao, J. *Ind. Eng. Chem. Res.* **1993**, *32*, 2826–2834.
(32) Aguado, R.; San Jose, M. J.; Olazar, M.; Alvarez, S.; Bilbao, J. *Chem. Eng. Process.* **2005**, *44*, 231–235.
(33) San José, M. J.; Olazar, M.; Peñas, F. J.; Arandes, J. M.; Bilbao, J. *Chem. Eng. Sci.* **1995**, *50*, 2161–2172.
(34) Makibar, J.; Fernandez-Akarregi, A. R.; Alava, I.; Cueva, F.; Lopez, G.; Olazar, M. *Chem. Eng. Process.* **2011**, DOI: 10.1016/J.cep2011.05.013.
(35) Calonaci, M.; Grana, R.; Hemings, E.; Bozzano, G.; Dente, M.; Ranzi, E. *Energy Fuels* **2010**, *24*, 5727–5734.
(36) Roy, C.; de Caumia, B.; Plante, P.; Ménard, H. *Proceedings of Energy from Biomass and Wastes VII*; Lake Buena Vista, FL, Jan 24−28, 1983; p 1147.
(37) Darmstadt, H.; Pantea, D.; Summchen, L.; Roland, U.; Kaliaguine, S.; Roy, C. *J. Anal. Appl. Pyrolysis* **2000**, *53*, 1–17.
(38) Boucher, M.; Chaala, A.; Pakdel, H.; Roy, C. *Biomass Bioenergy* **2000**, *19*, 351–361.
(39) Boucher, M.; Chaala, A.; Roy, C. *Biomass Bioenergy* **2000**, *19*, 337–350.
(40) Murwanashyaka, J.; Pakdel, H.; Roy, C. *J. Anal. Appl. Pyrolysis* **2001**, *60*, 219–231.
(41) Murwanashyaka, J.; Pakdel, H.; Roy, C. *Sep. Purif. Technol.* **2001**, *24*, 155–165.
(42) Garcia-Perez, M.; Chaala, A.; Roy, C. *J. Anal. Appl. Pyrolysis* **2002**, *65*, 111–136.
(43) Garcia-Perez, M.; Chaala, A.; Pakdel, H.; Kretschmer, D.; Roy, C. *J. Anal. Appl. Pyrolysis* **2007**, *78*, 104–116.
(44) Ba, T.; Chaala, A.; Garcia-Perez, M.; Rodrigue, D.; Roy, C. *Energy Fuels* **2004**, *18*, 704–712.
(45) Darmstadt, H.; Garcia-Perez, M.; Adnot, A.; Chaala, A.; Kretschmer, D.; Roy, C. *Energy Fuels* **2004**, *18*, 1291–1301.
(46) López, G.; Olazar, M.; Aguado, R.; Elordi, G.; Amutio, M.; Artetxe, M.; Bilbao, J. *Ind. Eng. Chem. Res.* **2010**, *49*, 8990–8997.
(47) Lopez, G.; Aguado, R.; Olazar, M.; Arabiourrutia, M.; Bilbao, J. *Waste Manage.* **2009**, *29*, 2649–2655.
(48) Olazar, M.; San Jose, M. J.; Aguayo, A. T.; Arandes, J. M.; Bilbao, J. *Ind. Eng. Chem. Res.* **1993**, *32*, 1245–1250.
(49) Olazar, M.; San Jose, M. J.; Llamosas, R.; Bilbao, J. *Ind. Eng. Chem. Res.* **1994**, *33*, 993–1000.
(50) Olazar, M.; Lopez, G.; Altzibar, H.; Aguado, R.; Bilbao, J. *Can. J. Chem. Eng.* **2009**, *87*, 541–546.
(51) Arabiourrutia, M.; Lopez, G.; Elordi, G.; Olazar, M.; Aguado, R.; Bilbao, J. *Chem. Eng. Sci.* **2007**, *62*, 5271–5275.
(52) Lopez, G.; Olazar, M.; Amutio, M.; Aguado, R.; Bilbao, J. *Energy Fuels* **2009**, *23*, 5423–5431.
(53) Artetxe, M.; Lopez, G.; Amutio, M.; Elordi, G.; Olazar, M.; Bilbao, J. *Ind. Eng. Chem. Res.* **2010**, *49*, 2064–2069.
(54) Elordi, G.; Olazar, M.; Lopez, G.; Artetxe, M.; Bilbao, J. *Ind. Eng. Chem. Res.* **2011**, *50*, 6650–6659.
(55) Elordi, G.; Olazar, M.; Lopez, G.; Artetxe, M.; Bilbao, J. *Ind. Eng. Chem. Res.* **2011**, *50*, 6061–6070.
(56) Altzibar, H.; Lopez, G.; Aguado, R.; Alvarez, S.; San José, M. J.; Olazar, M. *Chem. Eng. Technol.* **2009**, *32*, 463–469.
(57) San José, M. J.; Olazar, M.; Alvarez, S.; Izquierdo, M. A.; Bilbao, J. *Chem. Eng. Sci.* **1998**, *53*, 3561–3570.
(58) Gronli, M.; Varhegyi, G.; Di Blasi, C. *Ind. Eng. Chem. Res.* **2002**, *41*, 4201–4208.
(59) Garcia-Perez, M.; Adams, T.; Goodrum, J.; Geller, D.; Das, K. *Energy Fuels* **2007**, *21*, 2363–2372.
(60) Dupont, C.; Commandre, J.; Gauthier, P.; Boissonnet, G.; Salvador, S.; Schweich, D. *Fuel* **2008**, *87*, 1155–1164.
(61) White, J. E.; Catallo, W. J.; Legendre, B. L. *J. Anal. Appl. Pyrolysis* **2011**, *91*, 1–33.
(62) Cordero, T.; Garcia, F.; Rodriguez, J. J. *Therm. Acta* **1989**, *149*, 225–237.
(63) Cordero, T.; Rodriguez-Maroto, J. M.; Rodriguez, J. J. *Therm. Acta* **1990**, *164*, 135–144.
(64) Varhegyi, G.; Antal, M.; Jakab, E.; Szabo, P. *J. Anal. Appl. Pyrolysis* **1997**, *42*, 73–87.
(65) Caballero, J.; Conesa, J.; Font, R.; Marcilla, A. *J. Anal. Appl. Pyrolysis* **1997**, *42*, 159–175.
(66) Teng, H.; Wei, Y. *Ind. Eng. Chem. Res.* **1998**, *37*, 3806–3811.
(67) Branca, C.; Albano, A.; Di Blasi, C. *Thermochim. Acta* **2005**, *429*, 133–141.
(68) Di Blasi, C.; Branca, C. *Ind. Eng. Chem. Res.* **2000**, *39*, 2169–2174.
(69) Varhegyi, G.; Gronli, M.; Di Blasi, C. *Ind. Eng. Chem. Res.* **2004**, *43*, 2356–2367.
(70) Teng, H.; Lin, H.; Ho, J. *Ind. Eng. Chem. Res.* **1997**, *36*, 3974–3977.
(71) Turton, R.; Bailie, R. C.; Whiting, W. B.; Shaeiwitz, J. A. *Analysis, Synthesis and Design of Chemical Processes*; Prentice Hall: Upper Saddle River, NJ, 2003; p 344.

(72) Xu, Y.; Wang, T.; Ma, L.; Zhang, Q.; Wang, L. *Biomass Bioenergy* **2009**, *33*, 1030–1036.
(73) Petrov, N.; Budinova, T.; Razvigorova, M.; Parra, J.; Galiatsatou, P. *Biomass Bioenergy* **2008**, *32*, 1303–1310.
(74) Boroson, M.; Howard, J.; Longwell, J.; Peters, W.; Boroson, M.; Howard, J.; Longwell, J.; Peters, W. *AIChE J.* **1989**, *35*, 120–128.
(75) Yang, Z.; Zhang, B.; Chen, X.; Bai, Z.; Zhang, H. *J. Anal. Appl. Pyrolysis* **2009**, *81*, 243–246.
(76) Cao, N.; Darmstadt, H.; Soutric, F.; Roy, C. *Carbon* **2002**, *40*, 471–479.
(77) Lua, A.; Yang, T. *J. Colloid Interface Sci.* **2004**, *276*, 364–372.
(78) Ismadji, S.; Sudaryanto, Y.; Hartono, S.; Setiawan, L.; Ayucitra, A. *Bioresour. Technol.* **2005**, *96*, 1364–1369.